



**HAL**  
open science

## Recasting Wave Functions into Valence Bond Structures: A Simple Projection Method to Describe Excited States

Julien Racine, Denis Hagebaum-Reignier, Yannick Carissan, Stephane Humbel

### ► To cite this version:

Julien Racine, Denis Hagebaum-Reignier, Yannick Carissan, Stephane Humbel. Recasting Wave Functions into Valence Bond Structures: A Simple Projection Method to Describe Excited States. *Journal of Computational Chemistry*, 2016, 37 (8), pp.771-779. 10.1002/jcc.24267 . hal-01306875

**HAL Id: hal-01306875**

**<https://amu.hal.science/hal-01306875>**

Submitted on 14 Sep 2017

**HAL** is a multi-disciplinary open access archive for the deposit and dissemination of scientific research documents, whether they are published or not. The documents may come from teaching and research institutions in France or abroad, or from public or private research centers.

L'archive ouverte pluridisciplinaire **HAL**, est destinée au dépôt et à la diffusion de documents scientifiques de niveau recherche, publiés ou non, émanant des établissements d'enseignement et de recherche français ou étrangers, des laboratoires publics ou privés.

# Recasting wave functions into valence bond structures: a simple projection method to describe excited states

Julien Racine, Denis Hagebaum-Reignier, Yannick Carissan and Stéphane Humbel<sup>1</sup>

Correspondence to: Stéphane Humbel (E-mail: [stephane.humbel@univ-amu.fr](mailto:stephane.humbel@univ-amu.fr))

## ABSTRACT

A method is proposed to obtain coefficients and weights of Valence Bond determinants from Multi Configurational wave functions. This reading of the wave functions can apply to ground states as well as excited states. The method is based on projection operators. Both energetic and overlap-based criteria are used to assess the quality of the resulting VB wave function. The approach gives a simple access to a VB rewriting for low-lying states, and it is applied to the allyl cation, to the allyl radical and to the ethene (notably to the V-state). For these states, large overlap between VB and Multi Reference wave functions are easily obtained. The approach proves to be useful to propose an interpretation of the nature of the V-state of ethene.

---

<sup>1</sup>J. Racine, D. Hagebaum-Reignier, Y. Carissan, S. Humbel/Aix Marseille Université, CNRS, Centrale Marseille, iSm2 UMR 7313, 13397, Marseille, France

## Introduction

Obtaining chemically clear and relevant information from Molecular Orbitals (MO) wave functions, that are delocalized, is a vast domain where the ideas related to localization plays an important role.[1] All approaches in this field are based on the atomic concept. Density or charge analysis,[2][3][4][5][6] electronic density derivative analysis,[7][8][9][10][11][12] and even various Energy Decomposition Analysis,[13][14][15] all reside on the ground of atomic objects, as centroids or as basins. Self consistent non orthogonal Valence Bond (VB) Theory [16][17][18] and related approaches[19][20][21][22] also rely on atomic centroids, and among the variety of VB approaches,[23] we focussed particularly on the first type of approaches, those that can define strictly localized orbitals.

These orbitals are used to define bonds and lone pairs. A two-electron bond drawn between two atoms, A and B, in a Lewis structure, embeds a covalent and two ionic VB structures. This charge fluctuation is expressed on the basis of VB determinants, built on the corresponding atomic orbitals,  $a$  and  $b$ : dropping the

normalization,  $\Phi_{\text{cov}}^{VB} = |a\bar{b}| + |b\bar{a}|$ ,  $\Phi_{\text{ion1}}^{VB} = |a\bar{a}|$ ,

and  $\Phi_{\text{ion2}}^{VB} = |b\bar{b}|$ .

These strictly localized VB structures provide the basis of elegant interpretations on the very nature of bonding, of the structure of the molecules, and even of their reactivity.[24][25] This is particularly true for ground states, and occasionally for excited states.[26][27]

For most cases a small number of electrons are active (and considered as such in the VB formalism), while the inactive electrons can be described using inactive orbitals. Those inactive

orbitals have the same occupation number in all the VB structures. Here, the inactive orbitals will simply correspond to the  $\sigma$  skeleton of  $\pi$ -conjugated compounds. Inactive orbitals can indeed be orthogonal one to one another, and orthogonal to the active orbitals.

In the present contribution, we convert a MO wave function to a combination of Lewis or Valence Bond (VB) localized structures. Several methods have been proposed in this field, and one of the approaches that partly guided us is that of Hiberty and Leforestier, where Hartree-Fock (HF) and Configuration Interaction (CI) wave functions were rewritten as combination of VB structures, written in minimal basis set.[28] Multi Configurational Self Consistent Field (MCSCF) and Multi Reference Configuration Interaction (MRCI) methods give more precise results because they embed more electronic correlation. They can describe at least qualitatively any molecular system, including excited states, and they require more extended basis sets to reach a reasonable accuracy. We redefined the Hiberty-Leforestier scheme in such a way that virtually any basis set and any multi-determinantal wavefunction can be used. We thus considered correlated MO wave functions and projected them onto VB determinants. Our approach can also be linked to Cooper's or Hirao's CASVB methods,[29][30][31][32][33] which use non-singular transformations of the orbitals from multi configurational MO wave functions to obtain those of the VB determinants as well as the coefficients of the VB expansion. However, we assume here that the orbitals of the VB determinants are known, and we evaluate solely the coefficients of the VB wave function, from the MO wave function.

The paper is organized as follow: In the first part the projection scheme is described, then it is tested on two allyl cases (cation and radical),

and on the emblematic case of the V state of ethene.

## Methods

As stated above, our MO wave function can be any multi determinant wave function. It encompasses of course HF, but also virtually any MCSCF+CI wave function, such as CASSCF or RASSCF.[34] The VB wave function is also multi-determinantal but it uses a different basis. We write

$$\begin{aligned} |\Psi^{MO}\rangle &= \sum_{i=1}^m C_i |\Phi_i^{MO}\rangle \\ |\Psi^{VB}\rangle &= \sum_{k=1}^n c_k |\Phi_k^{VB}\rangle \end{aligned} \quad (1)$$

where MO Slater determinants ( $\Phi_i^{MO}$ ) are expanded on MOs that are orthogonal and delocalized over the different atoms. VBs structures ( $\Phi_k^{VB}$ ) are expanded on VB spin orbitals, that are localized on atoms, and are in principle non-orthogonal one to one another.[35] One can make either VB structures with strictly localized orbitals, or Lewis structures, with so-called Bond Distorted Orbitals (BDO).[36] In the later case, the BDOs are bi-occupied and can extend over two atoms. Both types of structures (VB and Lewis) will be labelled as  $\Phi_k^{VB}$  in the following.

While  $C_i$  and  $\Phi_i^{MO}$  are obtained from standard MO calculations, both  $c_k$  and  $\Phi_k^{VB}$  require a specific Valence Bond code.[37][38] In the following, we consider that the  $\Phi_k^{VB}$  are known and only the  $c_k$  need to be evaluated.

The assumption that the  $\Phi_k^{VB}$  are known makes sense if the VB orbitals can be somehow transferable from one system to another,

and/or from some state to another state.[15][39] Hence, the  $\Phi_k^{VB}$  can be optimized independently from the targeted state, and used as building blocks for the wave function of a targeted state (ground or excited state). If  $\Psi^{MO}$  and  $\Psi^{VB}$  describe the same state, we can write:

where  $N$  is a normalization factor and  $\Phi_{rest}$  spans the complementary of the space spanned by the basis of the VB structures (the  $\Phi_k^{VB}$  basis). We shall also consider that  $\varepsilon$  can be small, although it is not compulsory (*vide infra*).

Moreover, because  $\Phi_{rest}$  complements the  $\Phi_k^{VB}$  basis, we can write:

$$\langle \Phi_k^{VB} | \Phi_{rest} \rangle = 0, \quad \forall k$$

Finally, we multiply equation (2) on the left by each  $\langle \Phi_k^{VB} |$  of the basis, and we obtain the system of linear equations that can give the set of the  $\{c_k\}$ , within a renormalization factor:

$$\begin{cases} \langle \Phi_1^{VB} | \Psi^{MO} \rangle = N \left( \sum_{k=1}^n c_k \langle \Phi_1^{VB} | \Phi_k^{VB} \rangle \right) \\ \langle \Phi_2^{VB} | \Psi^{MO} \rangle = N \left( \sum_{k=1}^n c_k \langle \Phi_2^{VB} | \Phi_k^{VB} \rangle \right) \\ \vdots \\ \langle \Phi_n^{VB} | \Psi^{MO} \rangle = N \left( \sum_{k=1}^n c_k \langle \Phi_n^{VB} | \Phi_k^{VB} \rangle \right) \end{cases} \quad (3)$$

The matrix form of this problem is  $\mathbf{B} = \mathbf{x} \cdot \mathbf{S}$ , where  $\mathbf{B}$  is the MO wave function vector written

in the  $\Phi_k^{VB}$  basis (its  $l^{\text{th}}$  component writes

$$B_l = \langle \Phi_l^{VB} | \Psi^{MO} \rangle, \mathbf{x}$$
 is the desired  $\Psi^{VB}$

vector, written in the same basis, and  $\mathbf{S}$  is the overlap matrix between the VB structures (

$$S_{lk} = \langle \Phi_l^{VB} | \Phi_k^{VB} \rangle). \text{ We thus define the } P_l$$

operators that project on each of the  $\Phi_l^{VB}$

structures by their action on  $\Psi^{MO}$ :

$$P_l | \Psi^{MO} \rangle = | \Phi_l^{VB} \rangle \langle \Phi_l^{VB} | \Psi^{MO} \rangle. \text{ Hence, } \Psi^{MO}$$

is projected onto the  $\Phi_k^{VB}$  basis and gives the

*projected VB wave function*  $\Psi^{VB}$ .

The resolution of equation (3), to obtain the {

$c_k$ }, is done with the robust DGESV algorithm from the Lapack library.[40] It is interesting to note that equation (2) holds true even when  $\varepsilon$  is not small. For valence states, we can always define a complete VB basis that spans the space

of  $\Psi^{MO}$ , and  $\varepsilon$  is small. However,  $\varepsilon$  is larger when the basis set formed by the VB structures

is not adequately chosen to describe  $\Psi^{MO}$ , either because the structures are not relevant, or because some structures are missing. Hence, even in such a case, a VB wave function can be obtained by our approach, although the VB wave function thereby obtained might not adequately describe the starting MO wave function. In order to get some indication whether or not the VB wave function

corresponds to the starting  $\Psi^{MO}$ , we simply compute the overlap between them, equation (4). When  $\tau$  is close to 1 (100 % fit), the VB and the MO wave functions are identical, while, when it is close to 0 %, the VB and the MO wave functions are orthogonal one to the other. In

the following, this overlap is called the trust factor, and noted  $\tau$ :

$$\tau = \langle \Psi^{VB} | \Psi^{MO} \rangle \quad (4)$$

Although very simple, such a trust factor is seldom used to assess Valence Bond wave functions.[41][42] The *variations* of  $\tau$ , even more than its actual value will be used to check the usefulness of an additional VB structure. In the end, the weight of each V B structure can be obtained with the Coulson-Chirgwin[43] formula, which writes:

$$\omega_l = \sum_{k=1}^n c_l c_k S_{lk} \quad (5)$$

## Results

In this section we use our projection method on two classes of systems: primarily on the low laying states of allyls (cation and radical), and secondly on the ground and on an excited state of ethene. The allyl cases are possibly simple cases, but they give the opportunity to test how symmetry is accounted for while no constraint is provided. The ethene case is a reputedly difficult case from the MO point of view, and was recently considered at the Valence Bond level.[44]

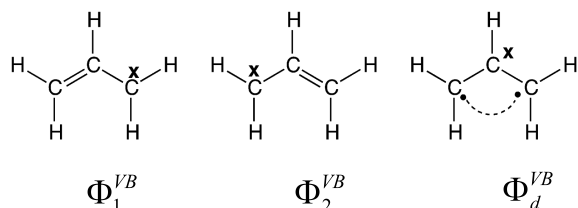
All calculations were carried out with GAMESS-US, version May 1 2013 (R1),[45] and XMVB 2.0 programs.[46] The 6-311+G(d) basis set,[47][48] with 6D cartesian primitives, as implemented by default in GAMESS-US, was used throughout. The allyls geometries were optimized at the B3LYP/6-311+G(d) level in the  $C_{2v}$  symmetry group,[49][50] while the geometry of the ethene is the experimental one.[51] More details can be found in the appendices and in Supporting Information.

## Allyls

The allylic systems can be described formally by a three-structure resonance; in two of them (Lewis structures) the double bond sits either

on the left ( $\Phi_1^{VB}$ ) or on the right ( $\Phi_2^{VB}$ ). These structures use BDO orbitals, extended on two atoms, to describe the  $\pi$  bond. A third structure must be added. It is a diradical VB

structure labelled  $\Phi_d^{VB}$ . [52][53] It is considered as a long-bond, and is drawn with a curly dash line to show that the two electrons are singlet-coupled. As each orbital is strictly localized on one atom, it corresponds to a VB structure rather than a Lewis structure. See Appendix 2 for more details on the VB orbital pre-optimization.

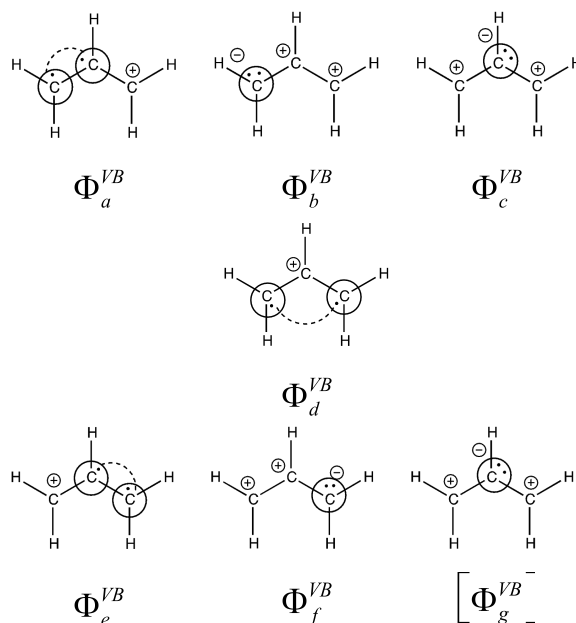


Scheme 1: Three-structure resonance for the allyl. The x symbol indicates the position of the charge, or of the radical dot.

### Allyl Cation

For the allyl cation, the x symbol in Scheme 1 indicates a positive charge, and the three structures are directly obtained from this scheme. In Lewis structures, the ionic/covalent ratio is biased. To discriminate covalent from ionic components, we can rewrite them as VB structures rather than Lewis': from  $\Phi_1^{VB}$  we generate  $\{\Phi_a^{VB}, \Phi_b^{VB}, \Phi_c^{VB}\}$ ,  $\Phi_2^{VB}$  to  $\{\Phi_e^{VB}, \Phi_f^{VB}, \Phi_g^{VB}\}$ , and the long bond structure  $\Phi_d^{VB}$

is retained as is. The redundancy  $\Phi_c^{VB} = \Phi_g^{VB}$  can be easily removed ( $\Phi_g^{VB}$  is in brackets in Scheme 2).



Scheme 2: VB structures for the allyl cation; the

brackets around  $\Phi_g^{VB}$  indicated that this structure is removed ( $\Phi_c^{VB} = \Phi_g^{VB}$ ). Circles represent atom-centered p orbitals.

We considered the first two singlet states of the allyl cation. CASSCF(2,3) calculations were used to describe both the  $^1A_1$  ground state and the

first  $^1B_2$  excited state. The  $\{\Phi_k^{VB}\}$  basis were obtained by standard VBSCF calculations of the ground state in three different cases: with only the Lewis structures  $\{\Phi_1^{VB}, \Phi_2^{VB}\}$  (noted  $\{\Phi_{1,2}^{VB}\}$ ), with the addition of the diradical structure  $\{\Phi_1^{VB}, \Phi_2^{VB}, \Phi_d^{VB}\}$  (or  $\{\Phi_{1,2,d}^{VB}\}$ ), and with the VB basis  $\{\Phi_a^{VB}, \Phi_b^{VB}, \Phi_c^{VB}, \Phi_d^{VB}, \Phi_e^{VB}, \Phi_f^{VB}\}$  (or  $\{\Phi_{a-f}^{VB}\}$ ).

As a result, we obtained for each case the coefficients ( $c_k$ ) of the projected wave function ( ), for the ground and for the excited states. These are not eigenvectors of

the VB Hamiltonian, so we computed the expectation value of the energy, which gives access to the energy difference between the two states ( $\Delta E$ , Table 1). The trust factor  $\tau$  (Equation 4) is reported as well.

Projected Wave function	$1^1A_1$ $\tau$ (%)	$1^1B_2$ $\tau$ (%)	$\Delta E$ (eV)
$\{\Phi_{1,2}^{VB}\}$	91	92	9.03
$\{\Phi_{1,2,d}^{VB}\}$	98	94	8.12
$\{\Phi_{a-f}^{VB}\}$	100	99	6.53
<b>CASSCF</b>	-	-	6.13

The trust factor is always close to 100%, so the projected wave functions adequately represent the physics of the corresponding state. For the

ground state, when  $\Phi_d^{VB}$  is included we notice a clear increase of the trust factor:  $\tau$  goes from 91% to 98%. It has been shown elsewhere that

$\Phi_d^{VB}$  plays indeed an important role on the resonance energy.[52][53] It is also shown that the basis of the VB structures is better than the Lewis ones and better balanced: the trust factor for the both ground and excited states is closed to 100% (100% and 99%), while when Lewis structures are used the trust factor for the excited state is a little smaller (94%). Only with this basis of VB structures is the energy difference between the two states reasonably good. The energy difference is then quite close to the CASSCF value (6.53 eV instead of 6.13 eV). In Lewis related basis, the energy difference between the two states is more than 2 eV too large: 8.12 eV instead 6.13 eV. This is to be attributed to the excited state, which has a too large energy. The energy criterion is obviously tougher than the trust factor, and the

error on  $\Delta E$  reminds us that orbital optimization can be required to obtain more accurate energies. However, the quality of the projected wave function is adequately gauged by  $\tau$ .

The projected wave functions can also be compared to actual eigenvectors of the Hamiltonian expressed on the basis of these VB

structures  $\{\Phi\}$ . Both ground and excited states are obtained without further modifying the VB structures, only the coefficients of the VB expansion are (slightly) different. In any case the projected functions and the eigenvectors are essentially the same (Table 2).

Projected		$C_1$	$C_a$	$C_b$	$C_c$	$C_d$
$\{\Phi_{1,2}^{VB}\}$	1					
	$1^1A_1$	0.55	-	-	-	-
	1	1.15	-	-	-	-
	$1^1B_2$					
$\{\Phi_{1,2,d}^{VB}\}$	1					
	$1^1A_1$	0.45	-	-	-	0.38
	1	1.08	-	-	-	0.00
	$1^1B_2$					
$\{\Phi_{a-f}^{VB}\}$	1					
	$1^1A_1$	-	0.42	0.03	0.23	0.34
	1	-	0.69	0.15	0.00	0.00
	$1^1B_2$					
<b>Eigenvecto</b>						
<b>r</b>						
$\{\Phi_{1,2}^{VB}\}$	1					
	$1^1A_1$	0.55	-	-	-	-
	1	1.15	-	-	-	-
	$1^1B_2$					
$\{\Phi_{1,2,d}^{VB}\}$	1					
	$1^1A_1$	0.45	-	-	-	0.38
	1	1.08	-	-	-	0.00
	$1^1B_2$					
$\{\Phi_{a-f}^{VB}\}$	1					
	$1^1A_1$	-	0.42	0.04	0.22	0.34
	1	-	0.69	0.15	0.00	0.00
	$1^1B_2$					

[a] We obtained with no symmetry constraint  $c_2 = c_1$  for the  $A_1$  state, and  $c_2 = -c_1$  for the  $B_2$  state. This is consistent with the

symmetry of the states. [b] We also obtained  $c_e = c_a$  and  $c_f = c_b$  for the  $A_1$  state, and  $c_e = -c_a$  and  $c_f = -c_b$  for the  $B_2$  state.

For instance with the two Lewis structures  $\{\Phi_{1,2}^{VB}\}$ :  $c_1=0.55$  for the  $A_1$  ground state and  $c_1=1.15$  for the  $B_2$  state are obtained by both the projected and the standard approaches. Hence, projected and eigenvectors are identical.

With  $\{\Phi_{1,2,d}^{VB}\}$ , the same is encountered ( $c_1, c_d$ )=(0.45, 0.38) for the ground state whatever the method we used (projected or eigenvectors). The same matching is seen for the excited state: ( $c_1, c_d$ )=(1.08, 0.00). Hence, the remaining defects of the projected wave function in these small basis is not due to the projection approach, but to the quality of the basis used for the structures, and notably to the VB orbitals.

The agreement between projected and eigenvectors is identically good when VB structures  $\{\Phi_{a-f}^{VB}\}$  are used instead of the Lewis ones. The coefficients ( $c_a, c_b, c_c, c_d$ ) displayed in Table 2 for both methods show very small differences.

### Allyl Radical

For the allyl radical, the  $\cdot$  symbol of scheme 1 indicates a radical dot, and, as it was the case for the cation, the three structures of Scheme 1 are directly obtained from this scheme. In the following we use for the structures the same notation as in the cation ( $\Phi_1^{VB}, \Phi_a^{VB}$  etc), but the structures are obviously different.

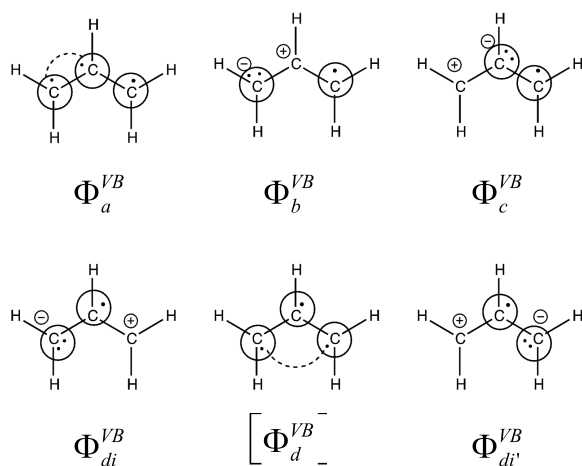
The Lewis structures can also be rewritten to obtain VB structures rather than Lewis ones (scheme 3:  $\Phi_1^{VB}$  corresponds to  $\{\Phi_a^{VB}, \Phi_b^{VB}, \Phi_c^{VB}\}$ , structure  $\Phi_2^{VB}$  to  $\{\Phi_e^{VB}, \Phi_f^{VB}, \Phi_g^{VB}\}$ .

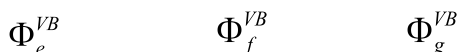
However, from the long bond structure  $\Phi_d^{VB}$  we can generate two new ionic structures

labelled  $\Phi_{di}^{VB}$  and  $\Phi_{di'}^{VB}$ . These ionic structures were obtained differently for the cation. Second difference with the cation, while no obvious redundancies appear, it is well established that  $\Phi_d^{VB}$  is redundant with  $\Phi_a^{VB}$  and  $\Phi_e^{VB}$ :  $\Phi_d^{VB} = \Phi_a^{VB} + \Phi_e^{VB}$ . [23] It is thus removed ( $\Phi_d^{VB}$  is in brackets in scheme 3).

We considered the two first doublet states of the allyl radical using CASSCF(3,3) calculations to describe both the  $^2A_2$  ground state and the first  $^2B_1$  excited state. [54][55] The basis were obtained by standard VBSCF calculations of the ground state in three different cases: with only the Lewis structures  $\{\Phi_1^{VB}, \Phi_2^{VB}\}$ , with  $\{\Phi_1^{VB}, \Phi_2^{VB}, \Phi_d^{VB}\}$ , and with the VB basis  $\{\Phi_a^{VB}, \Phi_b^{VB}, \Phi_c^{VB}, \Phi_{di}^{VB}, \Phi_{di'}^{VB}, \Phi_e^{VB}, \Phi_f^{VB}, \Phi_g^{VB}\}$ , which is noted  $\{\Phi_{a-g}^{VB}\}$ .

Again the trust factor is close to 100% for the two states, no matter if the Lewis structures are expanded as VB structures or not. The difference between the expectation values of the energy of the two states is comparable to that of the parent CASSCF wave functions (within 0.5 eV).





Scheme 3: VB structures for the allyl radical.

The brackets around  $\Phi_d^{VB}$  indicated that this structure is removed (see text). Circles represent atom-centered  $\pi$  orbitals.

It is interesting to note that, while structure  $\Phi_d^{VB}$  is redundant with  $\Phi_a^{VB}$  and  $\Phi_e^{VB}$ , it is not redundant with Lewis structures  $\Phi_1^{VB}$  and  $\Phi_2^{VB}$ . Indeed  $\tau$  is increased from 90% to 97% when  $\Phi_d^{VB}$  is added to the  $\{\Phi_1^{VB}, \Phi_2^{VB}\}$  basis. This can be attributed to a balancing of the ionic/covalent ratio, which is biased in  $\Phi_1^{VB}$  and in  $\Phi_2^{VB}$ .

Table 3. Trust factor ( $\tau$ ) and relative energy obtained for the projection of the CASSCF(3,3) wave function of the ground ( $1^2A_2$ ) or excited ( $1^2B_1$ ) states of the allyl radical, on different basis of localized structures.			
Projected Wave function	$1^2A_2$ $\tau$ (%)	$1^2B_1$ $\tau$ (%)	$\Delta E$ (eV)
$\{\Phi_1^{VB}, \Phi_2^{VB}\}$	99	90	5.57
$\{\Phi_1^{VB}, \Phi_2^{VB}, \Phi_d^{VB}\}$	99	97	3.78
<b>VB basis</b> $\{\Phi_{a-g}^{VB}\}$	100	98	3.88
<b>CASSCF</b>	-	-	3.39

Table 4. Allyl radical: coefficients of the projected wave functions compared to those of the eigenvectors computed in

the same basis of VB structures, with the same VB orbitals.[a,b]						
Projecte d		$c_1$	$c_a$	$c_b$	$c_c$	$c_d/c_d$
						i
$\{\Phi_{1,2}^{VB}\}$	$1^2A_2$	0.59	-	-	-	-
	$1^2B_1$	0.93	-	-	-	-
$\{\Phi_{1,2,d}^{VB}\}$	$1^2A_2$	0.59	-	-	-	0.00
	$1^2B_1$	-0.5	-	-	-	0.54
		1				
$\{\Phi_{a-g}^{VB}\}$	$1^2A_2$	-	0.46	0.12	0.09	0.05
	$1^2B_1$	-	0.89	0.17	0.11	0.05
<b>Eigen-ve ctor</b>						
$\{\Phi_{1,2}^{VB}\}$	$1^2A_2$	0.59	-	-	-	-
	$1^2B_1$	0.93	-	-	-	-
$\{\Phi_{1,2,d}^{VB}\}$	$1^2A_2$	0.59	-	-	-	0.00
	$1^2B_1$	-0.5	-	-	-	0.55
		0				
$\{\Phi_{a-g}^{VB}\}$	$1^2A_2$	-	0.41	0.16	0.12	0.07
	$1^2B_1$	-	0.92	0.19	0.09	0.05
[a] We obtained with no symmetry constraint $c_2 = -c_1$ for the $A_2$ state, and $c_2 = c_1$ for the $B_1$ state. This is consistent with the symmetry of the states. [b] We also obtained $c_e = -c_a$ , $c_f = -c_b$ , $c_g = -c_c$ and $c_{dir} = -c_{di}$ for the $A_2$ state, and the wave function is symmetric for the $B_1$ excited state.						

The projected VB wave functions are again very close to the actual eigenvectors of the VB Hamiltonian: this can be seen on the

coefficients of VB structures  $\{\Phi_{a-g}^{VB}\}$  ( $c_a, c_b, c_c, c_{di}$ ) displayed in Table 4. The very good match is again true for both ground and excited states. In Table 4 the numbers obtained by our projection scheme differ by at most 0.05 from that obtained variationally. For the ground state we get by projection  $c_a = 0.46$  while the variational number is  $c_a = 0.41$ . A similar accuracy is obtained for the excited state.

### Ethene

In the following, the ethene was considered in its experimental geometry,[51] and the  $D_{2h}$

symmetry notation applies.<sup>2</sup> In order to apply our projected method, we need to have a reasonably good MO wave function to start with. The literature on ethene's excited states, and particularly on the V state ( $1^1B_{1u}$ ), is very rich, and the recent paper published last year by Feller *et al.*[56] provides a detailed survey of the subject, particularly in their supporting information. To put it in a nutshell, the ground state ( $1^1A_g$ ) is called the N state, and the  $1^1B_{1u}$  excited state is called the V state.[56][57][58][59][60][61][44] The V state is reputedly difficult to describe due to some mixing with a Rydberg state of same symmetry ( $2^1B_{1u}$ ), and the starting orbitals are of great importance. Feller *et al.* provide an estimate of the Full CI/complete basis set limit for the vertical excitation energy, 8.02 eV,[56] in close agreement with others.[62][63][64][65][66][67] Finally, the best computations so far differ by about 0.3 eV.

The V state corresponds formally to a  $\pi \rightarrow \pi^*$  excitation. However, not only the  $\pi$  electrons, but also  $\sigma'$  ones have to be correlated to account for a so-called "dynamic  $\sigma$  polarization" mentioned by Angeli.[68] We used RAS+S wave functions (see Appendix 1), as in some of the Angeli's approaches. We also noted that the diffuseness of the V state is not very sensitive to the basis set:  $\langle x^2 \rangle$  varies by about  $0.5 a_0^2$  when the basis varies from double  $\zeta$  ( $2 \zeta$ ) to  $5 \zeta$ .[56] In these conditions, and considering that VB calculations will be involved and are meaningful in rather small basis sets, we restricted ourselves to the 6-311+G(d) basis set. Wu *et al.* used a similar basis set to study the V state at various VB levels, and they obtained values very consistent with the literature:  $\langle x^2 \rangle = 19.2 a_0^2$  and  $\Delta E_{N-V} = 7.97$  eV.[44]

Table 5. RAS results in the 6-311+G(d) basis set for the electronic states of ethene. N corresponds to the ground

state, V to the $1^1B_{1u}$ state. $V_R$ stands for the V state when it is contaminated by the Rydberg state.			
Level State	$n_{\text{Det}}$ [a]	$\langle x^2 \rangle$ [b]	$\Delta E$ [c]
RAS [2,2]			
$V_R$ :	66	22.29	11.90
V :	66	18.72	8.73
N :	68	11.70	0.00
RAS [2,6]			
$V_R$ :	678	22.42	11.24
V :	678	17.45	8.32
N :	684	11.79	0.00
[a] Number of determinant in the wave function. [b] Unit : $a_0^2$ . [c] Vertical excitation energy from the N state, in eV.			

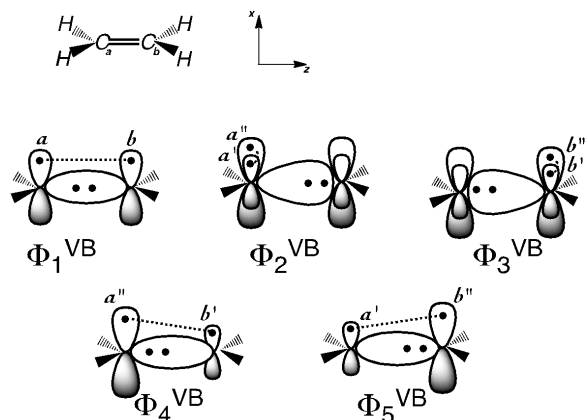
Our RAS+S wave functions for the pure V state, in such a small basis set, do not attempt to compete with the excellent work found in the literature, but, as shown in Table 5, they certainly carry the physics of the V state. Indeed, both the  $\langle x^2 \rangle$  and the vertical excitation energies are in the range of the best values of the literature.

#### Projection of the MO wave function onto VB

All the VB structures used for this study are gathered in Scheme 4. We have considered this ethene test case in the spirit of the recent Valence Bond study of Wu *et al.*,[44] and we shall particularly use the covalent structure they

introduced :  $\Phi_4^{VB}$  and  $\Phi_5^{VB}$ . The first three structures are the usual VB structures: covalent ( $\Phi_1^{VB}$ ), and ionics ( $\Phi_2^{VB}$  and  $\Phi_3^{VB}$ ).

<sup>2</sup> The molecule lies in the (y,z) plane. The two carbon atoms are on the z axis, and the  $\pi$  orbitals are defined by the  $p_{x_a}$  and  $p_{x_b}$  primitives of each carbon atom. See scheme 4.



Scheme 4: Lewis structure and all  $\Phi_k^{VB}$  structures for ethene.

In Scheme 4, we represent the  $\sigma$  system as a single orbital with two electrons. This orbital is polarized in  $\Phi_2^{VB}$  to illustrate the fact that the  $\sigma$  orbitals have been pre-optimized for this ionic structure. Indeed, the orbitals adapt to the charge situation of the  $\pi$  system, with a negatively charged carbon atom on the left hand side, while it is positively charged on the right hand side (see Appendix 2).

The  $\sigma$  orbitals are bi-occupied while the active  $\pi$  orbitals are mono-occupied. They are labelled  $a'$  and  $a''$  and are singlet coupled, as mentioned earlier. Because structure  $\Phi_1^{VB}$  is the symmetric covalent structure, its  $\sigma$  system is pictured with a symmetric bi-occupied orbital, and the  $a$  and  $b$  orbitals are pre-optimized for this symmetric occupation. Finally we shall emphasize that we use different orbitals for different configurations, in the spirit of the BOVB[16][17] approach:  $a \neq a' \neq a''$  and  $b \neq b' \neq b''$ . The orbitals for  $\Phi_4^{VB}$  and  $\Phi_5^{VB}$  are defined as follow:  $a', a'', b'$  and  $b''$  come from  $\Phi_2^{VB}$  and  $\Phi_3^{VB}$ . These  $\pi$  orbitals are frozen, while the  $\sigma$  orbitals have been re-optimized for

either  $\Phi_4^{VB}$  or for  $\Phi_5^{VB}$ . Accordingly, the  $\sigma$  orbitals of  $\Phi_4^{VB}$  and  $\Phi_5^{VB}$  look different.

#### Ground state of ethene

The two aforementioned MO wave functions have been used to describe the N state: RAS[2,2]+S or RAS[2,6]+S ( $\Psi^{MO}$ ). The different

sets of VB structures ( $\Phi_k^{VB}$ ) used for the projection on the N state are reported in Table 6 together with the trust factor and the relative energy. Except for the last entry, we used the RAS[2,2]+S wave function. The projection on three pre-optimized VB structures gives a high trust factor,  $\tau=97.7\%$ , and the expectation value of the energy of the projected wave function serves as a reference energy for the whole table. In the two entries that follow, the basis of the VB structures is biased, so the quality of the description is intentionally decreased, and we appraise the sensitivity of the trust factor to the quality of the basis of VB structures. When only the determinants of the covalent structure are used,  $\tau$  is only slightly lowered (95.6%) and the expectation value of the energy rises by +0.8 eV. These two variations are consistent but of different magnitude. It is interesting to note that when only the ionic structures are used  $\tau$  falls down to 83.9%, and the mean value of the energy rises significantly (+3.2 eV). It is a well-known fact that ionic structures do not suffice to describe such a covalent bond, and it is nice to see that our two indicators, the usual energetic one and the variation of  $\tau$ , make a clear signal of the misuse of the VB structures.

Table 6. Trust factor ( $\tau$ ) and relative energy obtained for the projection of the RAS[2,2]+S wave function of the N state of ethene on different VB wave functions.		
VB wave function	$\tau$ (%)	$\Delta E$ (eV)
$\{\Phi_1^{VB}, \Phi_3^{VB}\}$	97.7	0.0

$\{\Phi_1^{VB}\}$	95.6	+0.8
$\{\Phi_1^{VB}, \Phi_3^{VB}\}$	83.9	+3.2
$\{\Phi_1^{VB}, \Phi_3^{VB}\}$ [a]	99.1	-0.5
$\{\Phi_1^{VB}, \Phi_3^{VB}\}$ [b]	97.7	+0.1

[a] The VB orbitals are pre-optimized for the state rather than for single structures.  
[b] Projection scheme with the RAS[2,6]+S wave function.

In the next entry it is the RAS[2,6]+S wave function that is projected on the full set of pre-optimized VB structures. The results are similar to those obtained with the RAS[2,2]+S wave function:  $\tau$  is identical (97.7%), and the expectation value of the energies differ by a rather small value, about +0.1 eV. These two indicators tell that the two wave functions contain about the same physical meaning.

In the three first entries, the VB orbitals were pre-optimized for individual structures. In the fourth, the VB orbitals are pre-optimized for the N state and, as shown by the value of  $\tau$  (99.1%), the projected VB wave function gets a bit closer to  $\Psi^{MO}$ .

The VB coefficients and their corresponding weights are given in Table 7. The two determinants of the covalent wave function are in phase,<sup>3</sup> which is consistent with the g symmetry and with the singlet coupling of the ground state.

When the ionic structures are included, they are in phase (g symmetry). The coefficients and the weights of the various cases reported here differ by only a few %, which indicates that the projected wave function provides roughly the

<sup>3</sup> The inversion operator  $i$  applies to the  $\pi$  orbitals as follow:  $i(a)=-b$  and  $i(b)=-a$ . Hence  $i(i)=-(-)$ .

same physical meaning: the ground state is essentially covalent.

Table 7. Coefficients and weights of VB structures for the N state of ethene; projection of the RAS[2,2]+S wave function. Due to the symmetry of the N state,  $c_3=c_2$  and  $w_3=w_2$ .

VB wave function	$c^1$ ( $c^2$ )	$w_1$ ( $w_2$ )
$\{\Phi_1^{VB}, \Phi_3^{VB}\}$	0.76 (0.19)	73.9 (13.1)
$\{\Phi_1^{VB}, \Phi_3^{VB}\}$ [a]	0.78 (0.17)	76.9 (11.6)

[a] Projection scheme with the RAS[2,6]+S wave function.

### Excited state of ethene

The V state of ethene belongs to the  $B_{1u}$  symmetry. It is antisymmetric through the inversion operator  $i$ , so the standard singlet

coupled covalent VB wave function ( $\Phi_1^{VB}$  in Scheme 4) cannot be used anymore. Wu *et al.* introduced the covalent part of the V state with asymmetrical orbitals,  $a''$  and  $b'$  as in structure

for instance.[44] The out of phase

combination of  $a''$  and  $\Phi_5^{VB}$  is indeed antisymmetric.<sup>4</sup>

In Table 8, first entry, we obtained only  $\tau = 91.4\%$  and this value could be enhanced (up to 98.8%) when VB orbitals are pre-optimized for the V state (fourth entry). The difference between these cases is thus in the orbitals rather than in the projection scheme. Interestingly, when we remove some VB structures,  $\tau$  varies significantly (entry 2 and 3). For instance when only the ionics are used (entry 2),  $\tau$  drops down to 75.4%, and when only the covalent are used,  $\tau$  is as small to

<sup>4</sup> We have  $i(i)=-$  and  $i(-)=$ .

0.9%. The mean values of the energy are also subject to variations that are consistent with  $\tau$ .

Table 8. Trust factor ( $\tau$ ) and relative energy obtained for the projection of the RAS[2,2]+S wave function of the V state of ethene on different VB wave functions. The last column gives the vertical excitation energy.			
VB wave function	$\tau$ (%)	$\Delta E$ (eV)	$\Delta E_{N-V}$ (eV)
$\{ \Phi_1^{VB}, \Phi_3^{VB}, \Phi_5^{VB} \}$	91.4	0.0	+8.97
$\{ \Phi_2^{VB}, \Phi_3^{VB} \}$	75.4	+0.6	
$\{ \Phi_1^{VB}, \Phi_5^{VB} \}$	0.9	+8.0	
$\{ \Phi_1^{VB}, \Phi_3^{VB}, \Phi_5^{VB} \}$ [a]	98.8 %	-1.4	+8.10
$\{ \Phi_1^{VB}, \Phi_3^{VB}, \Phi_5^{VB} \}$ [b]	93.2	-0.3	+8.63

[a] The VB orbitals are pre-optimized for the V state rather than for single structures.  
[b] Projection scheme with the RAS[2,6]+S wave function.

The last entry concerns the projection of the RAS[2,6]+S wave function of the V-state onto the VB structures with pre-optimized orbitals. The results are very similar to the first entry of the table: the trust factors are within about 2% and the mean values of the energy are similar, within about  $\pm 0.3$  eV. The mean values obtained for the V state can be compared to that of the N state to find an estimate of the NV excitation energy. The values are reported in the last column: +8.97 eV with the projection of the RAS[2,2]+S wave functions, and +8.63 eV with the RAS[2,6]+S wave function. Again, the results are considerably enhanced when VB orbitals are pre-optimized for the V state (+8.10 eV, forth entry).

We report in Table 9 the coefficients and the weights obtained for the projected wave function. In the first entry, the covalent

structures ( $\Phi_1^{VB}$  and  $\Phi_5^{VB}$ ) have large coefficients ( $\pm 0.92$ ), but their Coulson-Chirgwin weights are very small. It is difficult to attribute this behaviour to a unique component. A large balance occurs, due to the sign alternation of the coefficients of similar magnitude, and to the fact that overlaps between structures are similar ( $S_{45} = 0.72$  and  $S_{43} = 0.73$ ). An extensive discussion on the weights in non-orthogonal CI can be read in a very interesting contribution of Thorsteinsson and Cooper.[69]

It shall be reminded that other definitions of the weights (Löwdin's or inverse-weights) can also be used. Wu *et al.* for instance used them,[44] but the weights attributed to these structures are still small compared to their role showed by the variations of  $\tau$  in Table 4. Indeed, when they are included in the basis of VB structures, the match between  $\Psi^{MO}$  and  $\Psi^{VB}$  is significantly better:  $\tau$  goes from 75.4% to 91.4%. These puzzling observations lead us to analyse the wave function in more detail, to better understand the role of the covalent structures.

Table 9. Coefficients and weights of VB structures for the V state of ethene; projection of the RAS[2,2]+S wave function. Due to the symmetry of the V state, $c_3 = -c_2$ , $c_5 = -c_4$ , and $w_3 = w_2$ , $w_5 = w_4$ .		
VB wave function	$c^2$ ( $c^4$ )	$w^2$ (%) ( $w^4$ )
$\{ \Phi_2^{VB}, \Phi_3^{VB}, \Phi_5^{VB} \}$	0.98 (0.92)	50.4 (-0.4)
$\{ \Phi_1^{VB}, \Phi_5^{VB} \}$ [a]	0.98 (0.80)	52.9 (-2.9)

[a] Projection scheme with the RAS[2,6]+S wave function.

### Role of covalent structures in the V-state

Our projection routines run primarily on the basis of the  $n_{\text{Det}}$  VB determinants ( $D_k^{VB}$ , Equation 6, Table 10) and these determinants are gathered in a (1,1) ratio to obtain structures ( , Equation 1), either ionic ( $\Phi_2^{VB}$  and  $\Phi_3^{VB}$ ), or covalent ( $\Phi_4^{VB}$  and  $\Phi_5^{VB}$ ). The ratio (and the sign) between the determinants has to be consistent with the spin coupling (singlet).

$$|\Psi^{VB}\rangle = \sum_{k=1}^{n_{\text{Det}}} d_k^{VB} |D_k^{VB}\rangle \quad (6)$$

Scheme 5: One electron bond through  $a'$  and  $b'$ .

A closer look at the wave function when it is written on the basis of these determinants (Table 10) suggests that a variety of couplings between determinants can be built, particularly those related to one-electron bonds. They correspond to an in-phase combination of two determinants where one of the two electrons swings between the two atoms, while the other settles in a fixed spin orbital. For instance we can consider that the first electron (of  $\alpha$  spin) swings between the two carbons using the  $a'$  and  $b'$  orbitals while the  $\beta$  electron settles on the left carbon atom, in the  $a''$  orbital (Scheme 5). For the sake of conciseness, we labelled

$\{\Psi_{\bar{a}''}^{1e}\}$  such a contribution. Hence, we extract un-normalized one-electron contributions from the wave function like:

$$\{\Psi_{\bar{a}''}^{1e}\} = 0.54D_1 + 0.60D_6.^5$$

<sup>5</sup> As a matter of fact, the lowest (normalized) eigenvector built on these two determinants describes a one-electron

Table 10. VB determinants for the V state of ethene and their coefficients in the projected wave function (RAS[2,2]+S).

$ D_k^{VB}\rangle$	$d_k^{VB}$
$D_1 =  a' \bar{a}''\rangle$	+0.54
$D_2 =  a'' \bar{a}'\rangle$	+0.54
$D_3 =  b' \bar{b}''\rangle$	-0.54
$D_4 =  b'' \bar{b}'\rangle$	-0.54
$D_5 =  a'' \bar{b}'\rangle$	+0.60
$D_6 =  b' \bar{a}''\rangle$	+0.60
	-0.60
$D_8 =  b'' \bar{a}'\rangle$	-0.60

The wave function can thus be rewritten as a combination of one-electron bond contributions (Equation 7),

$$\Psi^{VB} = N \left[ \{\Psi_{\bar{a}''}^{1e}\} + \{\Psi_{a''}^{1e}\} - \{\Psi_{\bar{b}''}^{1e}\} - \{\Psi_{b''}^{1e}\} \right] \quad (7)$$

where  $\{\Psi_{a''}^{1e}\}$ , built on  $D_2$  and  $D_5$  corresponds to spin switches from  $\{\Psi_{\bar{a}''}^{1e}\}$ . Similarly,

$\{\Psi_{b''}^{1e}\}$  is built on  $D_4$  and  $D_7$ , and  $\{\Psi_{\bar{b}''}^{1e}\}$  is built on  $D_3$  and  $D_7$ . Note the sign alternation

bond, as follow: . The coefficients are somehow similar to those of in the V state.

between  $\{\Psi_{\bar{a}^n}^{1e}\}$  and  $\{\Psi_{a^n}^{1e}\}$ , vs  $\{\Psi_{\bar{b}^n}^{1e}\}$  and  $\{\Psi_{b^n}^{1e}\}$ .

This rewriting embeds no additional approximation because the determinants are combined with the same coefficients as in Table 9. The trust factor is thus the same,  $\tau = 91.4\%$ . However, the new structures have now the

same weights:  $w_{a^n}^{1e} = w_{\bar{a}^n}^{1e} = w_{b^n}^{1e} = w_{\bar{b}^n}^{1e} = 25\%$ .

These new reading of the wave function is satisfactory for two reasons: (i) because the coefficients and the weights behave approximately the same, and (ii) because it gives a reasonable answer to the puzzling fact that the distorted long bonds are important, but have had negligible weights. As a result, the V state of ethylene can be considered as the out-of-phase combination of one-electron bonds, where one electron resides on one of the carbon while the other fluctuates between the two atoms.

In addition, the “one-electron interpretation” of the V-state might very well provide an interpretation of the large effects of dynamic correlation in the  $\sigma$  orbitals noted elsewhere.[44][56][61] Indeed, the hidden  $\pi$  electron fluctuation that occurs in the one-electron bonds must induce a dynamic  $\sigma$  orbitals repolarisation that requires to handle a significant part of  $\sigma$  correlation.

## Conclusions

In this paper, we presented a method to obtain coefficients and weights of a VB wave function from a MCSCF wave function. We also defined a trust factor  $\tau$  based on the overlap between the starting MCSCF wave function and the projected VB. We applied successfully this approach to ground and low-lying excited states

of three systems: allyl cation, allyl radical and ethene.

In the cases we considered, the nature of the projected wave function does not depend dramatically on the quality of the VB orbitals, and sound results are obtained even if orbitals are pre-optimized in a different context. The trust factor,  $\tau$  was used to get confidence in the resulting VB wave function to assess that it corresponds to the appropriate state described by the MR-CI computation. When the VB orbitals are pre-optimized for the targeted states,  $\tau$  increases moderately, and the energy differences get more accurate.

In our complete projection scheme, we not only obtain a wave function for a given state, we also associate it to a trust factor, which, in addition to the energy criterion, gives strong confidence (or warnings) about the relevance of the VB writing. It also serves as a guide to actually analyse the wave function in terms of local contributions. The approach is not restricted to the lowest states in their spin and symmetry. It can be applied to any state, provided a valid MO wave function can be defined in terms of Slater determinants. A complementary pedagogical version of this work is briefly sketched in appendix 3.

## Appendices

### 1. RASSCF wave functions

RAS[2,2]SCF + S wave function has two doubly occupied core orbitals:  $1a_g$ ,  $1b_{1u}$ , then five  $\sigma$  orbitals in the RAS 1 space:  $2a_g$ ,  $2b_{1u}$ ,  $1b_{2u}$ ,  $3a_g$ ,  $1b_{3g}$ . In RAS 2 space we used two  $\pi$  orbitals:  $1b_{3u}$ ,  $1b_{2g}$  and in RAS 3 space, we put five unoccupied  $\sigma$  orbitals:  $2b_{2u}$ ,  $3b_{1u}$ ,  $4a_g$ ,  $2b_{3g}$ ,  $4b_{1u}$ .

RAS[2,6]SCF + S wave function is similar to RAS[2,2]SCF + S wave function but with six  $\pi$  orbitals in RAS 2 space:  $1b_{3u}$ ,  $2b_{3u}$ ,  $3b_{3u}$ ,  $1b_{2g}$ ,  $2b_{2g}$ ,  $3b_{2g}$ .

For these two RAS wave functions: we used a maximum number of hole in RAS 1=1, in RAS 2=1, and a maximum number of particle in RAS 2=1, in RAS 3=1. Hence, only mono-excitations (hole-particle) are permitted.

## 2. VB wave functions

For all VB calculations, the  $2p_x$  active orbitals are optimized on the basis of the  $p_x$  and  $d_{xz}$  primitives of the same atom (i.e. the orbitals are optimized locally, and they can polarize). The active orbitals can be mono-occupied and singlet coupled to define a normalized two-determinantal covalent structure of the

type  $(a, b) = N'(|a\bar{b}| + |b\bar{a}|)$ . Ionic structures can be defined as either doubly occupied orbitals ( $a', a'$ ) or as splitted mono-occupied orbitals ( $a', a''$ ). They are of course also singlet coupled.

In the VB calculations (allyls and ethene), the  $\sigma$  orbitals are delocalized and orthogonal to each other. For the allyls the  $\sigma$  and  $\pi$  VB orbitals are optimized for the multi structure ground state using the VBSCF technique: all the structures share the same set of orbitals. For the ethene unless otherwise stated, they are obtained from a single  $\pi$  structure energy optimization. Hence, each structure has its own set of orbital.

## 3. Hückel related approach

The method we present here can be related to our Hückel-Lewis Projected method (HLP, HuLiS project), [70][71] where a noticeably reliable description of ground states in terms of local structures was obtained for “Hückel-compatible” systems. [72][73][74][75]

## Acknowledgments

Prof Wei Wu, and his team at Xiamen University, is gratefully acknowledged for the XMVB code. Dr Giard, Linares, Braïda and

Hiberty are acknowledged for advices, bibliographic support and related discussions.

**Keywords:** Electronic Structure . Bond Theory . Multi Reference . Excited States . Valence Bond

((Additional Supporting Information may be found in the online version of this article.))

## References and Notes

- [1] P. L. Ayers, R. J. Boyd, P. Bultinck, M. Caffarel, R. Carbo-Dorca, M. Causa, J. Cioslowski, J. Contreras-Garcia, D. L. Cooper, P. Coppens, C. Gatti, S. Grabowsky, P. Lazzeretti, P. Macchi, A. M. Pendas, P. L. A. Popelier, K. Ruedenberg, H. Rzepa, A. Savin, A. Sax, W. H. E. Schwarz, S. Shahbazian, B. Silvi, M. Sola, V. Tsirelson, *Comput. Theor. Chem.*, **2015**, 1053, 2 – 16.
- [2] R. S. Mulliken, *J. Chem. Phys.*, **1955**, 23, 1833–1840.
- [3] E. D. Glendening, F. Weinhold, *J. Comput. Chem.*, **1998**, 19, 593–609.
- [4] E. D. Glendening, C. R. Landis, F. Weinhold, *Wiley Interdiscip. Rev. Comput. Mol. Sci.*, **2012**, 2, 1–42.
- [5] E. D. Glendening, C. R. Landis, F. Weinhold, *J. Comput. Chem.*, **2013**, 34, 1429–1437.
- [6] A. Ikeda, Y. Nakao, H. Sato, S. Shige-yoshi, *Chem. Phys. Lett.*, **2011**, 505, 148–153.
- [7] R. F. W. Bader, *Acc. Chem. Res.*,

**1985**, *18*, 9–15.

[8] R. F. W. Bader, *Atoms in Molecules, Encyclopedia of Computational Chemistry*, 1. John Wiley & Sons, Ltd, Chichester, UK, 1998.

[9] A. D. Becke, K. E. Edgecombe, *J. Chem. Phys.*, **1990**, *92*, 5397–5403.

[10] H. L. Schmider, A. D. Becke, *J. Mol. Struct. THEOCHEM*, **2000**, *527*, 51 – 61.

[11] P. Karafiloglou, *J. Comput. Chem.*, **2001**, *22*, 306–315.

[12] M. Menéndez, A. Martín Pendás, B. Braïda, A. Savin, *Comput. Theor. Chem.*, **2015**, *1053*, 142 – 149.

[13] G. Frenking, K. Wichmann, N. Frohlich, C. Loschen, M. Lein, J. Frunzke, V. Rayon, *Coord. Chem. Rev.*, **2003**, *238*, 55–82.

[14] A. Krapp, F. M. Bickelhaupt, G. Frenking, *Chem.- Eur. J.*, **2006**, *12*, 9196–9216.

[15] N. J. Mayhall, P. R. Horn, E. J. Sundstrom, M. Head-Gordon, *Phys Chem Chem Phys*, **2014**, *16*, 22694–22705.

[16] P. C. Hiberty, S. Humbel, C. P. Byrman, J. H. van Lenthe, *J. Chem. Phys.*, **1994**, *101*, 5969–5976.

[17] P. C. Hiberty, S. S. Shaik, *Theor. Chim. Acta*, **2002**, *108*, 255–272.

[18] W. Wu, P. Su, S. Shaik, P. C. Hiberty,

*Chem. Rev.*, **2011**, *111*, 7557–7593.

[19] W. J. Hunt, P. J. Hay, W. A. G. Iii, *J. Chem. Phys.*, **1972**, *57*, 738–748.

[20] D. L. Cooper, J. Gerratt, M. Raimondi, *Modern Valence Bond Theory, Advances in Chemical Physics: Ab Initio Methods in Quantum Chemistry Part 2*, 69. John Wiley & Sons, Inc., Hoboken, New Jersey, USA, 1987.

[21] D. L. Cooper, P. B. Karadakov, B. J. Duke, *J. Phys. Chem. A*, **2015**, *119*, 2169–2175.

[22] C. Angeli, R. Cimiraglia, J.-P. Malrieu, *J. Chem. Educ.*, **2008**, *85*, 150–158.

[23] S. S. Shaik, P. C. Hiberty, in *A Chemist's Guide to Valence Bond Theory*; John Wiley & Sons, Inc., Hoboken, New Jersey, USA, **2007**.

[24] S. S. Shaik, A. Shurki, *Angew. Chem. Int. Ed.*, **1999**, *38*, 586–625.

[25] A. Shurki, E. Derat, A. Barrozo, S. C. L. Kamerlin, *Chem. Soc. Rev.*, **2015**, *44*, 1037–1052.

[26] D. Usharani, W. Lai, C. Li, H. Chen, D. Danovich, S. Shaik, *Chem. Soc. Rev.*, **2014**, *43*, 4968–4988.

[27] H. Zhang, D. Danovich, W. Wu, B. Braïda, P. C. Hiberty, S. Shaik, *J. Chem. Theory Comput.*, **2014**, *10*, 2410–2418.

[28] P. C. Hiberty, C. Leforestier, *J. Am. Chem. Soc.*, **1978**, *100*, 2012–2017.

- [29] T. Thorsteinsson, D. L. Cooper, J. Gerratt, P. B. Karadakov, M. Raimondi, *Theor. Chim. Acta*, **1996**, *93*, 343–366.
- [30] T. Thorsteinsson, D. L. Cooper, *Int. J. Quantum Chem.*, **1998**, *70*, 637–650.
- [31] T. Thorsteinsson, D. L. Cooper, J. Gerratt, M. Raimondi, *Theor. Chim. Acta*, **1997**, *95*, 131–150.
- [32] K. Hirao, H. Nakano, K. Nakayama, M. Dupuis, *J. Chem. Phys.*, **1996**, *105*, 9227–9239.
- [33] H. Nakano, K. Nakayama, K. Hirao, *J. Mol. Struct. THEOCHEM*, **1999**, *461*, 55 – 69.
- [34] J. Olsen, B. O. Roos, P. Jorgensen, H. J. A. Jensen, *J. Chem. Phys.*, **1988**, *89*, 2185–2192.
- [35] R. Pauncz, in *The Construction of Spin Eigenfunctions. An exercise book*; Kluwer Academic/Plenum Publishers, New York, USA, **2000**.
- [36] Y. Mo, Z. Lin, W. Wu, Q. Zhang, *J. Phys. Chem.*, **1996**, *100*, 11569–11572.
- [37] L. Song, Z. Chen, F. Ying, J. Song, X. Chen, P. Su, Y. Mo, Q. Zhang, W. Wu, in *XMVB*; Xiamen University, Xiamen 361005, China, **2012**.
- [38] L. Song, Y. Mo, Q. Zhang, W. Wu, *J. Comput. Chem.*, **2005**, *26*, 514–521.
- [39] M. Sironi, A. Genoni, M. Civera, S. Pieraccini, M. Ghitti, *Theor. Chem. Acc.*, **2007**, *117*, 685–698.
- [40] Univ. of Tennessee, Univ. of California Berkeley, Univ. of Colorado Denver and NAG Ltd., LAPACK version 3.5.0. 2011.
- [41] T. Thorsteinsson, D. Cooper, *Theor. Chim. Acta*, **1996**, *94*, 233–245.
- [42] D. M. Hirst, J. W. Linnett, *J. Chem. Phys.*, **1965**, *43*, S74–S79.
- [43] B. H. Chirgwin, C. A. Coulson, *Proc. R. Soc. Lond. Math. Phys. Eng. Sci.*, **1950**, *201*, 196–209.
- [44] W. Wu, H. Zhang, B. Braïda, S. Shaik, P. C. Hiberty, *Theor. Chem. Acc.*, **2014**, *133*, 1–13.
- [45] M. W. Schmidt, K. K. Baldridge, J. A. Boatz, S. T. Elbert, M. S. Gordon, J. H. Jensen, S. Koseki, N. Matsunaga, K. A. Nguyen, S. Su, T. L. Windus, M. Dupuis, J. A. Montgomery, *J. Comput. Chem.*, **1993**, *14*, 1347–1363.
- [46] L. Song, J. Song, Y. Mo, W. Wu, *J. Comput. Chem.*, **2009**, *30*, 399–406.
- [47] R. Krishnan, J. S. Binkley, R. Seeger, J. A. Pople, *J. Chem. Phys.*, **1980**, *72*, 650–654.
- [48] T. Clark, J. Chandrasekhar, G. W. Spitznagel, P. V. R. Schleyer, *J. Comput. Chem.*, **1983**, *4*, 294–301.
- [49] S. H. Vosko, L. Wilk, M. Nusair, *Can. J. Phys.*, **1980**, *58*, 1200–1211.
- [50] A. D. Becke, *Phys. Rev. A*, **1988**, *38*, 3098–3100.
- [51] G. Herzberg, in *Electronic spectra*

and electronic structure of polyatomic molecules; Van Nostrand, Princeton, New Jersey, USA, **1966**.

[52] M. Linares, B. Braïda, S. Humbel, *J. Phys. Chem. A*, **2006**, *110*, 2505–2509.

[53] M. Linares, S. Humbel, B. Braïda, *J. Phys. Chem. A*, **2008**, *112*, 13249–13255.

[54] I. Fischer, *Chem. Soc. Rev.*, **2003**, *32*, 59–69.

[55] L. Castiglioni, A. Bach, P. Chen, *Phys. Chem. Chem. Phys.*, **2006**, *8*, 2591–2598.

[56] D. Feller, K. A. Peterson, E. R. Davidson, *J. Chem. Phys.*, **2014**, *141*, 104302.

[57] S. Krebs, R. J. Buenker, *J. Chem. Phys.*, **1997**, *106*, 7208–7214.

[58] T. Müller, M. Dallos, H. Lischka, *J. Chem. Phys.*, **1999**, *110*, 7176–7184.

[59] R. McDiarmid, On the Electronic Spectra of Small Linear Polyenes, *Advances in Chemical Physics*. John Wiley & Sons, Inc., Hoboken, New Jersey, USA, 177–214, 1999.

[60] J.-P. Malrieu, N. Guihéry, C. Jiménez Calzado, C. Angeli, *J. Comput. Chem.*, **2007**, *28*, 35–50.

[61] C. Angeli, *Int. J. Quantum Chem.*, **2010**, *110*, 2436–2447.

[62] B. Lasorne, M. A. Robb, H.-D. Meyer, F. Gatti, *Chem. Phys.*, **2010**, *377*, 30–45.

[63] J. Watts, S. Gwaltney, R. Bartlett, *J.*

*Chem. Phys.*, **1996**, *105*, 6979–6988.

[64] P. G. Szalay, R. J. Bartlett, *Chem. Phys. Lett.*, **1993**, *214*, 481–488.

[65] J. R. Platt, H. B. Klevens, H. B. Price, *J. Chem. Phys.*, **1949**, *17*, 466–469.

[66] R. S. Mulliken, *J. Chem. Phys.*, **1977**, *66*, 2448–2451.

[67] J. P. Götze, B. Karasulu, W. Thiel, *J. Chem. Phys.*, **2013**, *139*, 234108.

[68] C. Angeli, *J. Comput. Chem.*, **2009**, *30*, 1319–1333.

[69] T. Thorsteinsson, D. L. Cooper, *J. Math. Chem.*, **1998**, *23*, 105–126.

[70] Y. Carissan, D. Hagebaum-Reignier, N. Goudard, S. Humbel, *J. Phys. Chem. A*, **2008**, *112*, 13256–13262.

[71] Y. Carissan, D. Hagebaum-Reignier, N. Goudard, S. Humbel, in *HuLiS Code: Lewis embedded in Hückel Theory*, **2008**.

[72] M. A. Fox, F. A. Matsen, *J. Chem. Educ.*, **1985**, *62*, 477–485.

[73] R. D. Harcourt, *J. Mol. Struct. THEOCHEM*, **1985**, *23*, 235–247.

[74] I. Maki, K. Kitaura, K. Nishimoto, *Theor. Chim. Acta*, **1994**, *89*, 89–104.

[75] Y. Mo, Q. Zhang, *Int. J. Quantum Chem.*, **1995**, *56*, 19–26.



## GRAPHICAL ABSTRACT

### AUTHOR NAMES

J. Racine, D. Hagebaum-Reignier, Y. Carissan, S. Humbel

### TITLE

Recasting wave functions into valence bond structures: a simple projection method to describe excited states

### TEXT

We formulate a bridge between Molecular Orbitals and Valence Bonds wave functions, for both ground and excited states. The approach is shown on calculations that embed Multi References and the Configuration Interaction of Singles and Double excitations. The overlap is used to assess that the VB description corresponds indeed to the MO's. The cases of allyl (cation or radical) and of the V state of ethene are used.

### GRAPHICAL ABSTRACT FIGURE

